MOLECULAR ENDOCRINOLOGY

Hydrocortisone and Purinergic Signaling Stimulate Sodium/Iodide Symporter (NIS)-Mediated Iodide Transport in Breast Cancer Cells

Orsolya Dohán, Antonio De la Vieja and Nancy Carrasco

Mol. Endocrinol. 2006 20:1121-1137 originally published online Jan 26, 2006; , doi: 10.1210/me.2005-0376

0888-8809/06/$15.00/0
Printed in U.S.A.

Molecular Endocrinology 20(5):1121–1137

doi: 10.1210/me.2005-0376

Hydrocortisone and Purinergic Signaling Stimulate Sodium/Iodide Symporter (NIS)-Mediated Iodide Transport in Breast Cancer Cells

Orsolya Dohán, Antonio De la Vieja, and Nancy Carrasco

Department of Molecular Pharmacology, Albert Einstein College of Medicine, Bronx, New York 10461

The sodium/iodide symporter (NIS) mediates a remarkably effective targeted radioiodide therapy in thyroid cancer; this approach is an emerging candidate for treating other cancers that express NIS, whether endogenously or by exogenous gene transfer. Thus far, the only extrathyroidal malignancy known to express functional NIS endogenously is breast cancer. Therapeutic efficacy in thyroid cancer requires that radioiodide uptake be maximized in tumor cells by manipulating well-known regulatory factors of NIS expression in thyroid cells, such as TSH, which stimulates NIS expression via cAMP. Similarly, therapeutic efficacy in breast cancer will likely depend on manipulating NIS regulation in mammary cells, which differs from that in the thyroid. Human breast adenocarcinoma MCF-7 cells modestly express endogenous NIS when treated with all-*trans*-retinoic acid (tRa). We report here that hydrocortisone and ATP each markedly stimulates tRa-induced NIS protein expression and plasma membrane targeting in MCF-7 cells, leading to at least a 100% increase in iodide uptake. Surprisingly, the adenyl cyclase activator forskolin, which promotes NIS expression in thyroid cells, markedly decreases tRa-induced NIS protein expression in MCF-7 cells. Isobutylmethylxanthine increases tRa-induced NIS expression in MCF-7 cells, probably through a purinergic signaling system independent of isobutylmethylxanthine's action as a phosphodiesterase inhibitor. We also observed that neither iodide, which at high concentrations down-regulates NIS in the thyroid, nor cAMP has a significant effect on NIS expression in MCF-7 cells. Our findings may open new strategies for breast-selective pharmacological modulation of functional NIS expression, thus improving the feasibility of using radioiodide to effectively treat breast cancer. (*Molecular Endocrinology* 20: 1121–1137, 2006)

A MAJOR DRAWBACK OF available traditional cytotoxic anticancer therapies is that they are significantly toxic to normal cells as well. Therefore, the ultimate aim of any new anticancer therapy is to achieve selective destruction of cancerous tissue with minimal harm to healthy cells. One of the most promising approaches to accomplishing this goal is targeted radiation therapy. In recent years, radionuclide-bearing monoclonal antibodies (mAbs) have been approved by the United States Federal Drug Administration, and several other antibodies (Abs) are currently on clinical trials. These mAbs bind to tumor-specific antigens, thus selectively targeting cytotoxic radionuclides to the tumor (1). Alternatively, cytotoxic radionuclides can be specifically targeted by acting as substrates of transport proteins that are selectively expressed in tumoral tissue. These transport proteins then translocate the radionuclides into tumoral cells only.

The prime example of targeted radiation therapy via a selectively expressed plasma membrane transporter is radioiodide therapy. This is the most effective anticancer targeted radiotherapy available today (2) and has been employed for more than 60 yr to destroy thyroid cancer remnants and/or metastases after thyroidectomy (3). The presence of the sodium/iodide symporter (NIS) in thyroid cancer cells ensures that administered radioiodide is selectively accumulated in these cells, causing little damage to other cells and only minimal side effects (2). Thus far, radioiodide therapy has been viewed as applicable only to thyroid cancer. Nevertheless, recent observations have raised the possibility of applying radioiodide therapy to breast cancer (4–6), and potentially to other cancers as well, by introducing NIS into the tumor via viral vectors (7–9) or up-regulating the tumors' endogenous NIS expression, if present (2, 4, 10, 11).

NIS was cloned in 1996 in our laboratory from the highly functional rat thyroid-derived FRTL-5 cells (12). It was subsequently demonstrated that the same NIS protein mediates I^- transport in all tissues that con-

First Published Online January 26, 2006

Abbreviations: Abs, Antibodies; 8-Br-cAMP, 8-bromo-cAMP; FACS, fluorescence-activated cell sorting; HBSS, Hank's balanced salt solution; IBMX, isobuthylmethylxantine; mAbs, monoclonal antibodies; NIS, sodium/iodide symporter; NUE, NIS upstream enhancer; PBS-C-M, PBS containing 0.1 mM $CaCl_2$ and 1 mM $MgCl_2$; tRA, all-*trans*-retinoic acid; tRAH, hydrocortisone combined with tRA.

***Molecular Endocrinology* is published monthly by The Endocrine Society (http://www.endo-society.org), the foremost professional society serving the endocrine community.**

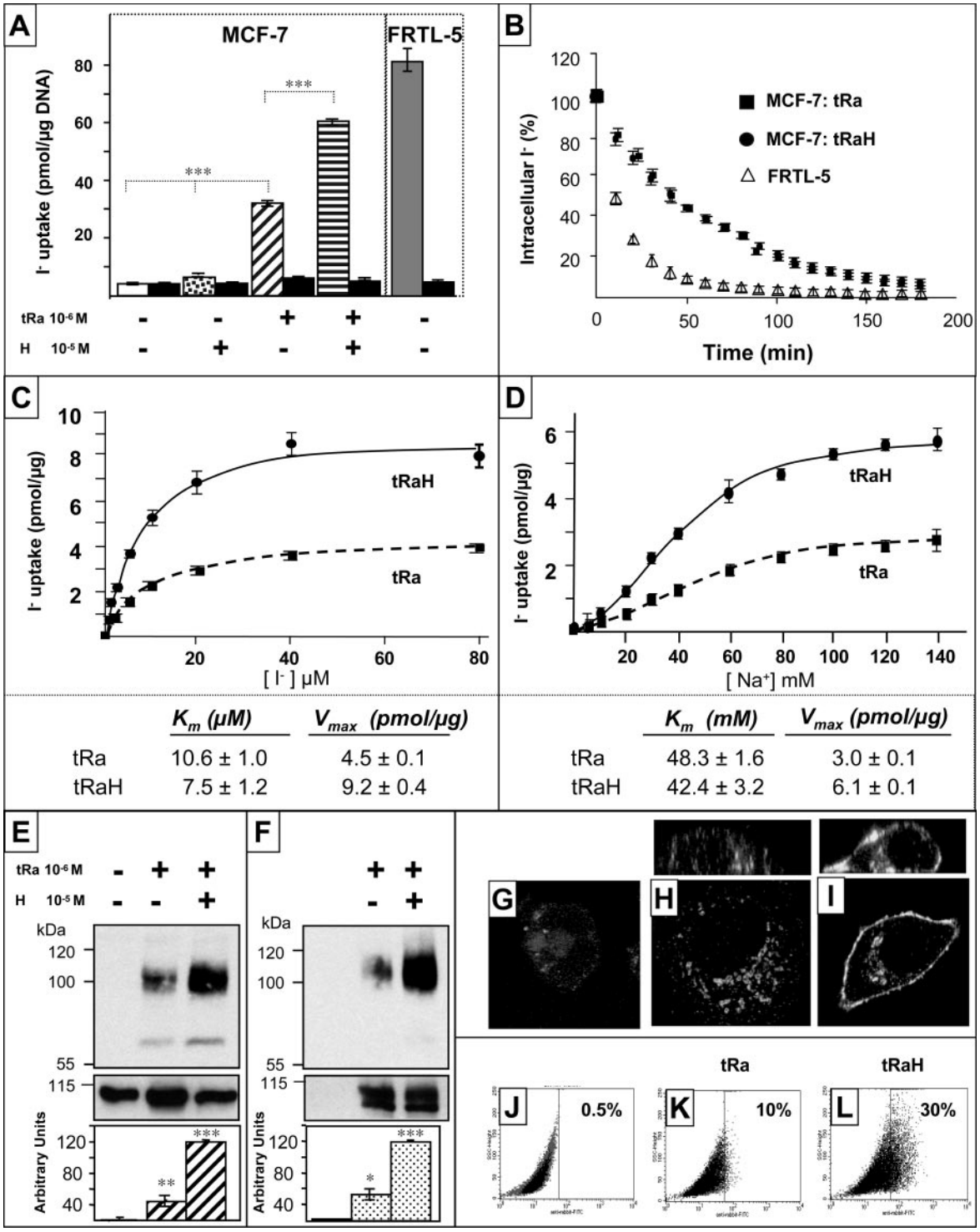

Fig. 1. Hydrocortisone Increases tRa-induced Functional NIS Expression in MCF-7 Cells

A, Steady-state I^- uptake in MCF-7 cells: nontreated (*white bar*); treated for 48 h with 10 μM hydrocortisone (H) (*spotted bar*), 1 μM tRa (*diagonally striped bar*), or tRa and H combined (*horizontally striped bar*). Cells were incubated for 30 min with 20 μM $Na^{125}I$ and assayed as described in *Materials and Methods.* For comparison, I^- uptake in FRTL-5 cells is shown (*gray bar*). *Black bars* represent $NaClO_4$ (40 μM) inhibition of I^- uptake in all cases. B, I^- efflux in MCF-7 cells treated with either tRa or tRaH is similar and significantly slower than in FRTL-5 cells. Cells were incubated with 20 μM $Na^{125}I$ for 30 min and washed; I^- efflux was measured by replacing the HBSS solution every 10 min for 3 h and quantitating ^{125}I. ■, tRa-treated MCF-7 cells; ●, tRaH-treated MCF-7 cells; △, FRTL-5 cells. C and D, Hydrocortisone increases the V_{max} of NIS-mediated I^- transport in tRa-treated MCF-7 cells without changing the K_m of the transporter for either I^- (panel C) or Na^+ (panel D). Initial rates (2-min time points) of I^- uptake were determined at the indicated concentrations of I^- (as described in *Materials and Methods*). Calculated curves were generated

centrate I^-, including salivary glands, gastric mucosa, and lactating mammary gland (4, 13, 14). Interestingly, NIS is regulated differently in each of these tissues (4, 14, 15). Our secondary structure model for NIS predicts 13 transmembrane segments (16); we have experimentally demonstrated that the amino terminus faces extracellularly and the carboxy terminus faces intracellularly (17).

Driven by the Na^+ gradient generated by the Na^+/K^+ ATPase, NIS couples the inward downhill transport of Na^+ down its concentration gradient to the inward uphill translocation of I^- against its electrochemical gradient. NIS transports 2 Na^+ per each I^- (18). Importantly, in addition to radioiodide, NIS also transports other radionuclides with high therapeutic potential, such as $^{188}ReO_4$ (19) and ^{211}At (20).

We have demonstrated in healthy mammary tissue that NIS is expressed in lactating but not in nonlactating breast and have shown that NIS expression is regulated by lactogenic hormones (4). By comparison, in the thyroid NIS is expressed continuously and is primarily regulated by TSH (14, 15, 17). We have observed NIS-mediated I^- uptake in mammary adenocarcinomas in transgenic mice bearing ras or neu oncogenes and, even more significantly, we found NIS expression in more than 80% of human breast cancers by immunohistochemistry (4, 6, 21), whereas there was no NIS expression in the surrounding noncancerous breast tissue. In short, some regulatory mechanisms cause NIS to be expressed only in lactating breast and breast cancer but not in noncancerous nonlactating breast. Furthermore, we have recently demonstrated *in vivo* that NIS-mediated I^- uptake occurs in human breast cancer metastases, and that thyroidal I^- uptake can be selectively down-regulated by administering thyroid hormones, which suppress TSH production in the anterior hypophysis (6). This would protect the thyroid from radioiodide administered to destroy breast cancer cells. To reach maximal therapeutic efficiency, patients with metastatic thyroid disease are given a low iodide diet and recombinant TSH (22). This greatly increases functional NIS expression and radioiodide accumulation in malignant thyroid tissue. Similarly, it is imperative to find comparable ways to selectively induce or increase existing endogenous functional NIS expression in breast cancer. Kogai *et al.* (11) have reported the induction of functional NIS expression by all-*trans*-retinoic acid (tRa) in the human adenocarcinoma-derived MCF-7 cell line. MCF-7 cells are an excellent and widely used *in vitro* system for studying NIS regulation in human breast cancer cells. Here we analyzed the effects of hormones and other factors on NIS expression in MCF-7 cells. We found that glucocorticoids and purinergic regulatory mechanisms greatly enhanced tRa-induced functional NIS expression in MCF-7 cells. Interestingly, factors that increased NIS expression in MCF-7 cells have the opposite effect in FRTL-5 cells, *i.e*. they down-regulate NIS expression. Our findings open new strategies for carrying out selective pharmacological modulation of radioiodide uptake in breast cancer.

RESULTS

Hydrocortisone Increases tRa-Induced Iodide Uptake in MCF-7 Cells

The combination of insulin, prolactin, and hydrocortisone induces the synthesis of milk proteins such as caseins and whey proteins in mammary epithelial cells *in vitro* (23–25). Having shown *in vivo* that NIS is expressed in the breast exclusively during pregnancy and lactation (4), we investigated whether lactogenic hormones modulate NIS protein synthesis in MCF-7 cells. Given that insulin is a required factor in the MCF-7 cell growth medium, we evaluated the effects

with the equation $v = V_{max}\cdot[I]/(K_m+[I])$, using Gnuplot software. Cells were incubated for 2 min with the indicated concentrations of Na^+; isotonicity was maintained constant with choline chloride. Na^+ dependence data were analyzed with the equation $v = V_{max}\cdot [Na^+]^2/K_m+[Na^+]^2)$. Data were fitted by nonlinear least squares using Gnuplot software. E, Total NIS protein expression in nontreated, tRa-, or tRaH-treated (48 h) MCF-7 cells. Experiments were performed at least in triplicate; representative data are shown. *Upper panel*, MCF-7 cells were treated for 48 h with 1 μM tRa or with the combination of 1 μM tRa and 10 μM hydrocortisone (panel H). Cells were lysed and subjected to immunoblot analysis with 4 nM anti-hNIS Ab. Total protein (20 μg) was loaded onto each lane. *Middle panel*, Equal loading was assessed by reprobing the same blot with an Ab against the α-subunit of the Na^+/K^+ ATPase. *Bottom panel*, NIS protein expression was quantitated using ImageQuant software and standardized for the loading control. F, Plasma membrane targeting of NIS in treated and nontreated MCF-7 cells. *Upper panel*, Immunoblot analysis of biotinylated cell surface polypeptides using 4 nM anti-hNIS Ab was carried out as described in *Materials and Methods. Middle panel*, Immunoblot analysis of biotinylated cell surface polypeptides, using an Ab against the α-subunit of the Na^+/K^+ ATPase. *Bottom panel*, NIS plasma membrane localization was quantified by densitometry using ImageQuant software and standardized for plasma membrane-localized α-subunit of the Na^+/K^+ ATPase. G–I, NIS expression analyzed by indirect immunofluorescence. Lack of NIS expression in nontreated MCF-7 cells (panel G); intracellular and faint plasma membrane-localized NIS expression in tRa-treated MCF-7 cells (panel H); clear plasma membrane localization of NIS in tRaH-treated MCF-7 cells (panel I). Cells were incubated with 4 nM anti-hNIS Ab and subsequently with a fluorescent isothiocyanate-labeled antirabbit IgG (Vector laboratories) as described in *Materials and Methods.* J–L, Quantitation of NIS-expressing MCF-7 cells before (panel J) and after treatment (48 h) with either tRa (panel K) or tRaH (panel L). Cells were probed first with 4 nM anti-hNIS Ab and subsequently with a fluorescent isothiocyanate-labeled anti-rabbit IgG. The fluorescence of 10,000 cells per tube and percentage of NIS-expressing MCF-7 cells were determined by a FACScan flow cytometer (Becton Dickinson and Co.) (see *Materials and Methods* for details).

of hydrocortisone (10 μM) and human recombinant prolactin (10 ng/ml), either alone or in combination, on steady-state I^- uptake. All experiments were performed in the presence of 2.5% charcoal-treated fetal bovine serum and 10 μg/ml insulin; steady-state perchlorate-sensitive I^- uptake was measured 48 h after each treatment. Neither hydrocortisone nor prolactin, alone or together, induced I^- uptake in MCF-7 cells in the absence of tRa (data not shown). However, hydrocortisone, when administered in combination with tRa (tRaH), caused a 2-fold increase in I^- uptake (Fig. 1A, *horizontally striped bar*) when compared with tRa treatment alone (Fig. 1A, *diagonally striped bar*), leading to I^- accumulation levels comparable to those in thyroid cells (Fig. 1A, *gray bar*). In contrast, prolactin, even at doses as high as 100 ng/ml to 1 μg/ml, had no effect on steady-state I^- uptake in cells simultaneously treated with either tRa alone or tRaH (data not shown).

Steady-state I^- uptake is the result of I^- influx, mediated by NIS, and I^- efflux, mediated by unidentified channels or transporters. Hence, we measured both I^- efflux and initial rates (2 min) of I^- uptake to determine which of these two components is (or are) modulated by hydrocortisone. For the efflux experiments, cells were allowed to reach steady state; I^- was then washed from the medium, thus causing intracellular I^- to efflux as a result of the outwardly directed I^- gradient. I^- efflux rates were exactly the same in tRa- and tRaH-treated MCF-7 cells, although these rates were considerably slower than those in FRTL-5 cells (Fig. 1B). These findings indicate that hydrocortisone increases tRa-induced I^- accumulation in MCF-7 cells solely by increasing NIS-mediated I^- transport, without affecting I^- efflux.

To further explore the effect of different hormonal treatments on NIS function in MCF-7 cells, we performed kinetic analyses of NIS-mediated I^- uptake (Fig. 1, C and D). We measured the effect of varying concentrations of I^- (ranging from 0.625 to 80 μM) on the initial rates (2 min) of I^- transport (Fig. 1C). In all cases saturation was reached at an I^- concentration of approximately 40 μM. The apparent V_{max} value of NIS was significantly higher (2-fold) when the combined tRaH treatment was used, as compared with tRa alone [$V_{max\ (I^-tRa)} = 4.5 \pm 0.1$; $V_{max\ (I^-tRaH)} = 9.2 \pm 0.4$ pmol I^-/μg DNA/2 min]. In contrast, the calculated Michaelis-Menten constant (K_m) values for I^- were similar in both conditions [$K_{m\ (I^-tRa)} = 7.5 \pm 1.2$; $K_{m\ (I^-tRaH)} = 10.6 \pm 1.0$ μM]. We also investigated the effect of varying concentrations of Na^+ (ranging from 0–140 mM) on initial I^- uptake rates in MCF-7 cells treated with either tRa or tRaH (Fig. 1D). Osmolarity was kept constant with choline chloride. We found that, similar to I^-, the K_m of NIS for Na^+ was the same in cells subjected to either treatment [$K_{m\ (Na^+-tRa)} = 48.3 \pm 3.2$, $K_{m\ (Na^+-tRaH)} = 42.4 \pm 1.6$ mM], whereas the V_{max} of Na^+ transport was also increased 2-fold [$V_{max\ (Na^+-tRa)} = 3.0 \pm 0.1$, $V_{max\ (Na^+-tRaH)} = 6.1 \pm 0.1$ pmol I^-/μg DNA/2 min] when the combined treatment was employed. These data suggest that the addition of hydrocortisone to tRa results in the presence of more functional NIS molecules in the plasma membrane of MCF-7 cells.

The Combination of tRa and Hydrocortisone Stimulates NIS Protein Expression and Targeting to the Plasma Membrane

Having established that the combination of tRa and hydrocortisone increases I^- uptake, we sought to discern the underlying mechanism involved. We assessed NIS expression and its subcellular localization in MCF-7 cells treated with either tRa alone or tRaH (Fig. 1, E–I). When present, the NIS protein migrated as an approximately 100-kDa mature and an approximately 60-kDa partially glycosylated polypeptide (17), as determined by immunoblot analysis (Fig. 1E). We found that both NIS protein expression and targeting to the plasma membrane increased significantly in cells treated with the tRaH combination compared with those treated with tRa alone (Fig. 1, E–F). NIS targeting to the plasma membrane was assessed by surface biotinylation experiments carried out with the amino-specific membrane-impermeable reagent Sulfo-NHS-SS-biotin. The entire biotinylated fraction was isolated with streptavidin-coated beads and immunoblotted with anti-hNIS Ab. Whereas an approximately 100-kDa immunoreactive band corresponding to mature NIS was evident in the immunoblot, the approximately 60-kDa partially glycosylated band was not observed because it does not reach the plasma membrane (Fig. 1F). Prolactin had no effect on NIS protein expression, independently of whether it was added alone or together with the tRaH combination (data not shown).

The MCF-7 cell line is heterogeneous (26). Hence, whereas NIS was clearly revealed by immunofluorescence to be localized in the plasma membrane of tRaH-treated MCF-7 cells (Fig. 1I), not all cells expressed NIS. By flow cytometry [fluorescence-activated cell sorting (FACS)], we quantitated the percentage of cells expressing NIS after hormonal treatment (Fig. 1, J–L), and observed that tRa induced NIS expression in only 10% of the cells (Fig. 1K). By comparison, the tRaH combination induced NIS expression in as many as 30% of the cells (Fig. 1L), indicating that the addition of hydrocortisone led not only to higher protein levels in tRa-responsive MCF-7 cells, but also enhanced the stimulatory effect of tRa. Virtually identical results were obtained with two other Abs directed against different NIS epitopes.

We determined the time course and dose dependence of the hydrocortisone effect on tRa-induced I^- uptake and NIS protein expression in MCF-7 cells (Fig. 2). The presence of 10 μM hydrocortisone for more than 12 h significantly increased I^- uptake (Fig. 2, A and B), NIS protein expression (Fig. 2, C and D), and plasma membrane targeting (Fig. 2, E and F). Incubation times up to 48 h resulted in no further increase in

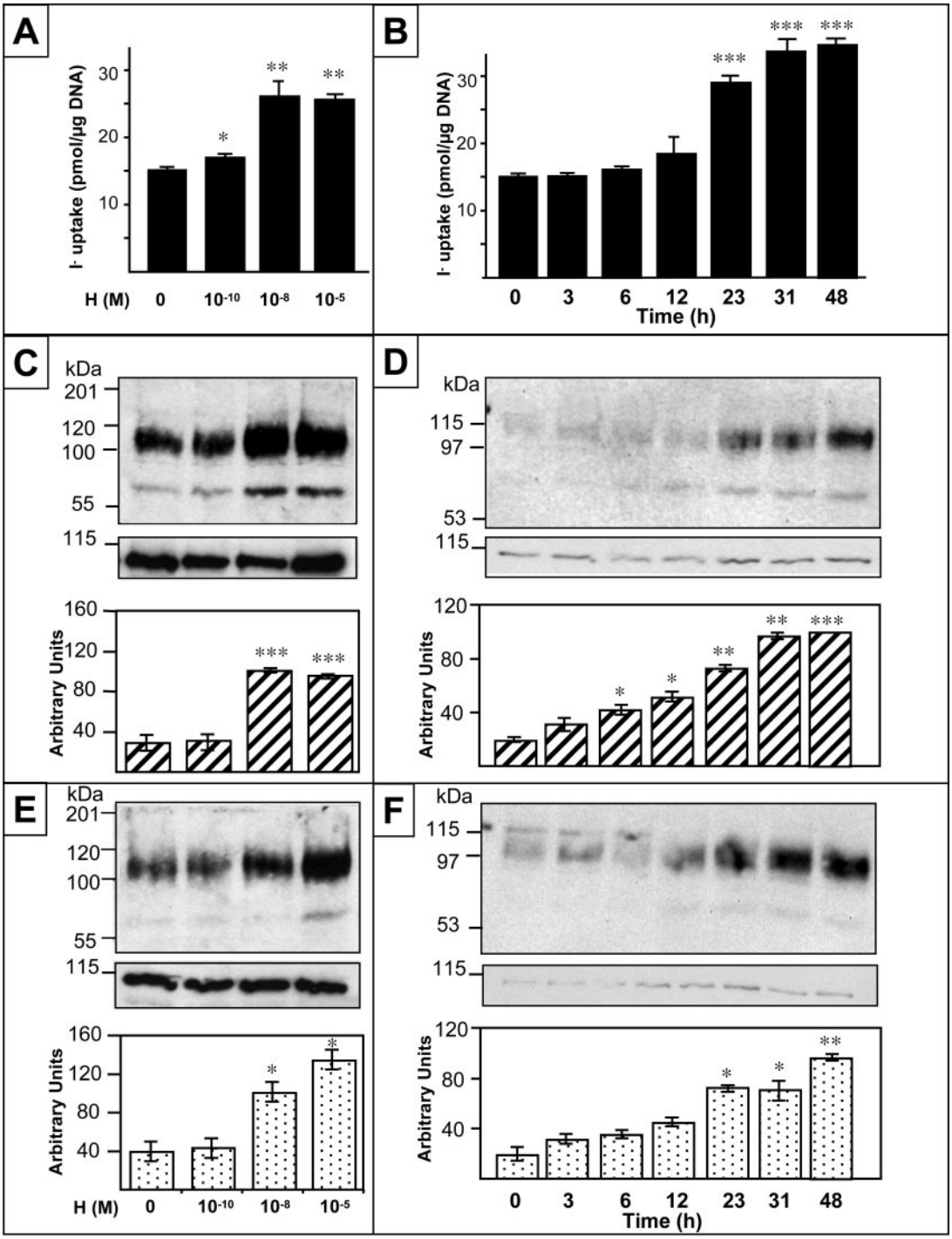

Fig. 2. Hydrocortisone Increases tRa-Induced NIS Expression in MCF-7 Cells in a Dose- and Time-Dependent Fashion

A**,** Steady-state I^- uptake in tRa-maintained (10^{-6} M) MCF-7 cells treated with increasing doses of hydrocortisone, or B**,** with 10^{-5} M hydrocortisone for the indicated times. For uptake measurements, cells were incubated in the presence of 20 μM $Na^{125}I$ for 30 min as described in *Materials and Methods*. C and D (*upper panels*), Immunoblot analysis of hNIS expression after hydrocortisone administration at the indicated concentrations for 48 h; 20 μg of total protein were loaded per lane (panel C), and after the administration of 10 μM hydrocortisone for the indicated times; 10 μg of total protein were loaded per lane (panel D). *Middle panels*, Loading control (Na^+/K^+ ATPase α-subunit). *Bottom panel*, The relative expression levels of hNIS, compared with the housekeeping protein Na^+/K^+ ATPase α-subunit, were quantified by densitometry using ImageQuant software. E–F (*upper panels*), Immunoblot analysis of biotinylated cell surface polypeptides with anti-hNIS polyclonal Ab after hydrocortisone administration at the indicated concentrations for 48 h (panel E), and after the administration of 10 μM hydrocortisone for various time lengths (panel F). *Middle panels*, loading control (Na^+/K^+ ATPase α-subunit). *Bottom panels*, hNIS plasma membrane localization was quantified by densitometry using ImageQuant software and standardized for plasma membrane-localized α-subunit of the Na^+/K^+ ATPase. H, Hydrocortisone.

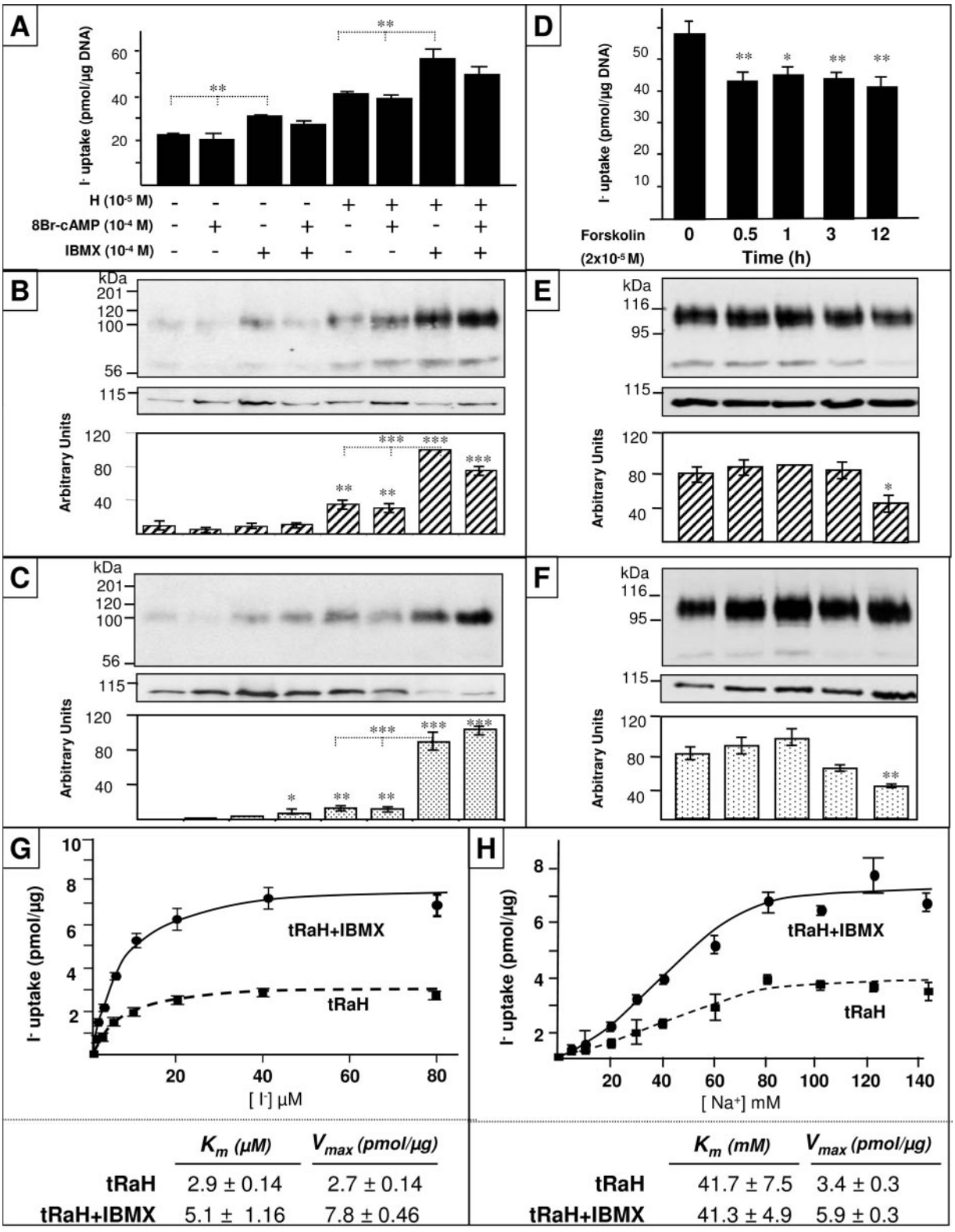

	K_m (µM)	V_{max} (pmol/µg)
tRaH	2.9 ± 0.14	2.7 ± 0.14
tRaH+IBMX	5.1 ± 1.16	7.8 ± 0.46

	K_m (mM)	V_{max} (pmol/µg)
tRaH	41.7 ± 7.5	3.4 ± 0.3
tRaH+IBMX	41.3 ± 4.9	5.9 ± 0.3

Fig. 3. IBMX Increases, whereas Forskolin Decreases Functional NIS Expression in tRaH-Treated MCF-7 Cells

A, Effect of 8-Br-cAMP and IBMX on steady-state I^- uptake in MCF-7 cells treated for 48 h with tRaH. Cells were incubated for 30 min with 20 µM $Na^{125}I$ and assayed as described in *Materials and Methods.* B, Total NIS protein expression in MCF-7 cells after administration of tRaH plus 8-Br-cAMP and/or IBMX for 48 h. *Upper panels*, MCF-7 cells were treated for 48 h with the combination of 1 µM tRa and 10 µM hydrocortisone (H) and with 100 µM 8-Br-cAMP or 100 µM IBMX, as indicated. Cells were lysed and subjected to immunoblot analysis with 2 nM anti-hNIS Ab. Total protein (20 µg) was loaded onto each lane. *Middle*

NIS protein expression and I^- uptake (Fig. 2). In the presence of tRaH, I^- uptake and NIS protein expression were maintained at a constant level, even after 6 d of treatment (data not shown). In contrast to hydrocortisone, none of the other lactogenic hormones with known roles in NIS regulation in mammary glands in mice, namely oxytocin, prolactin, and estrogen, alone or in combination, induced NIS expression or had any effect on tRa- or tRaH-induced NIS expression or NIS trafficking, or on I^- uptake in MCF-7 cells (data not shown). Insulin or IGF-I treatment resulted in a slight decrease of tRa- or tRaH-induced I^- uptake (data not shown).

Isobutylmethylxanthine (IBMX), but not cAMP, Stimulates I^- Uptake in tRa- and tRaH-Treated MCF-7 Cells

The regulation of NIS by TSH in the thyroid is mediated by cAMP (14, 15, 27, 28). Both the rat and human NIS gene 5′-untranslated regions contain a basic proximal promoter and an upstream enhancer (NUE = NIS upstream enhancer) that recapitulates the most relevant aspects of NIS regulation (28, 29). NUE, in turn, is composed by a degenerate cAMP-responsive element sequence flanked by two Pax8 binding sites. In the thyroid, the binding of both Pax8 and an unidentified cAMP-responsive element-like element binding factor to NUE is required to obtain full TSH/cAMP-dependent NIS transcription (28, 29). Given that cAMP plays a central role in the regulation of thyroid NIS, we investigated the effect of cAMP on NIS expression in MCF-7 cells by adding 100 μM 8-bromo-cAMP (8-Br-cAMP) (a membrane-permeable cAMP analog) to untreated or tRaH-treated MCF-7 cells. To slow down degradation of cAMP, the phosphodiesterase inhibitor IBMX was also added (100 μM). Not only did cAMP have no stimulatory effect but it had a slight inhibitory effect on I^- uptake in treated (tRa or tRaH) cells (Fig. 3A). Surprisingly, IBMX by itself caused a significant increase ($\sim$30%) of I^- uptake in both tRa- and tRaH-treated MCF-7 cells (Fig. 3A). Immunoblot and surface biotinylation experiments also showed that the tRaH-IBMX treatment resulted in both higher overall NIS protein expression and a higher number of NIS molecules in the plasma membrane, as compared with tRaH-treated cells (Fig. 3, B and C).

Kinetic analysis of I^- transport revealed that the addition of IBMX to tRaH led to the presence of more functionally active NIS molecules in the plasma membrane of MCF-7 cells (Fig. 3, G and H). The K_m values of NIS for both I^- and Na^+ were very similar [$K_{m\ (I^-tRaH)}$ = 2.89 $\pm$ 0.76 μM; $K_{m\ (I^-tRaH\text{-}IBMX)}$ = 5.1 $\pm$ 1.16 μM $K_{m\ (Na^+tRaH)}$ = 41.7 $\pm$ 7.5 mM; $K_{m\ (Na^+tRaH\text{-}IBMX)}$ = 41.28 $\pm$ 4.9 mM], whereas the V_{max} values for both I^- and Na^+ increased significantly when IBMX was added along with tRaH [$V_{max\ (I^-tRaH)}$ = 2.67 $\pm$ 0.14 pmol; $V_{max\ (I^-tRaH\text{-}IBMX)}$ = 7.82 $\pm$ 0.46 pmol; $V_{max\ (Na^+tRaH)}$ = 3.44 $\pm$ 0.28 pmol; $V_{max\ (Na^+tHRa\text{-}IBMX)}$ = 5.98 $\pm$ 0.34 pmol].

Although forskolin (20 μM) (an adenyl cyclase agonist) induces functional NIS expression in TSH-deprived FRTL-5 cells (27, 30), it significantly decreased tRaH-induced NIS activity in MCF-7 cells, even after a short administration (30 min) (Fig. 3D). These results are different from the lack of effect of forskolin in MCF-7 cells reported by Kogai *et al.* (10).

ATP Increases I^- Uptake in tRaH-Treated MCF-7 Cells

That cAMP slightly decreased IBMX stimulation of tRaH-induced I^- uptake and forskolin decreased tRaH-induced I^- uptake suggested that the IBMX ef-

panels, Equal loading was assessed by reprobing the same blot with an Ab against the α-subunit of the Na^+/K^+ ATPase. *Bottom panel*, NIS protein expression was quantitated using ImageQuant software and standardized for the loading control. C, Plasma membrane targeting of NIS in MCF-7 cells treated as described in panel B. *Upper panel*, Immunoblot analysis of biotinylated cell surface polypeptides, using 2 nM anti-hNIS Ab, carried out as described in *Materials and Methods. Middle panel*, Immunoblot analysis of biotinylated cell surface polypeptides with an Ab against the α-subunit of the Na^+/K^+ ATPase. *Bottom panel*, NIS plasma membrane localization was quantified by densitometry using ImageQuant software and standardized for plasma membrane-localized α-subunit of the Na^+/K^+ ATPase. D, Steady-state I^- uptake of tRaH-treated MCF-7 cells after administration of 20 μM forskolin for the indicated times. Cells were incubated for 30 min with 20 μM $Na^{125}I$ and assayed as described in *Materials and Methods.* E, Total NIS protein expression in MCF-7 cells in tRaH-treated MCF-7 cells after forskolin administration. *Upper panel*, MCF-7 cells were treated for 48 h with tRaH plus 20 μM forskolin for the indicated times. *Middle panel*, Equal loading was assessed by reprobing the same blot with an Ab against the α-subunit of the Na^+/K^+ ATPase. *Bottom panel*, NIS protein expression was quantitated using ImageQuant software and standardized for the loading control. F, Plasma membrane targeting of NIS in tRaH- and forskolin-treated MCF-7 cells. *Upper panels*, Immunoblot analysis of biotinylated cell surface polypeptides using 4 nM anti-hNIS Ab, carried out as described in *Materials and Methods. Middle panel*, Immunoblot analysis of biotinylated cell surface polypeptides, using an Ab against the α-subunit of the Na^+/K^+ ATPase. *Bottom panel*, NIS plasma membrane localization was quantified by densitometry using ImageQuant software and standardized for plasma membrane-localized α-subunit of the Na^+/K^+ ATPase. G, IBMX significantly increases the V_{max} of NIS-mediated I^- transport in tRaH-treated MCF-7 cells without changing the K_m of the transporter for I^- or Na^+ (panel H). Initial rates (2-min time points) of I^- uptake were determined at the indicated concentrations of I^- as described in *Materials and Methods*. Calculated curves were generated using the equation $v = V_{max}\cdot[I]/(K_m+[I])$ with Gnuplot software. H, To assess Na^+ dependence of I^- uptake, cells were incubated for 2 min with the indicated concentrations of Na^+; isotonicity was maintained constant with choline chloride. Na^+ dependence data were analyzed using the equation $v = V_{max}\cdot [Na^+]^2/K_m+[Na^+]^2$. Data were fitted by nonlinear least squares using the Gnuplot software.

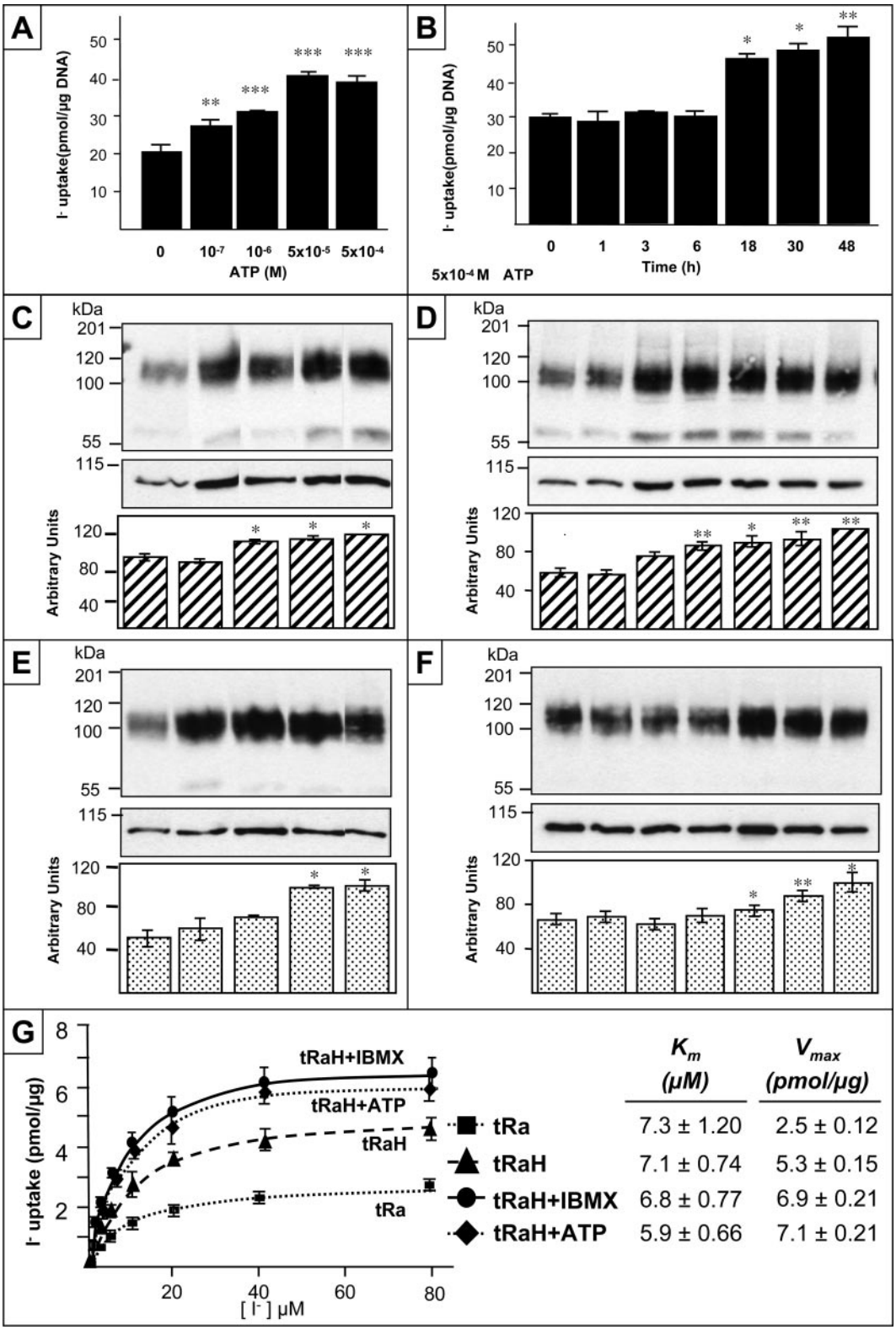

Fig. 4. ATP Increases I^- Uptake in tRaH-Treated MCF-7 Cells in a Dose- and Time-Dependent Manner

A and B, Steady-state I^- uptake in tRaH-maintained MCF-7 cells treated with the indicated concentrations of ATP for 48 h (panel A) or with 5×10^{-4} M ATP for the indicated times (panel B). Cells were incubated for 30 min with 20 μM $Na^{125}I$ and assayed as described in *Materials and Methods.* C and D, Total NIS protein expression in tRaH- and ATP-treated MCF-7 cells. *Upper panels*, MCF-7 cells were treated with tRaH and with the indicated concentrations of ATP for 48 h (panel C), or with 5×10^{-4} M ATP for the indicated times (panel D). Cells were lysed and subjected to immunoblot analysis using 2 nM anti-hNIS Ab. Total

fect was independent of the intracellular levels of cAMP. 8-Br-cGMP (up to 500 μM) had no effect on tRaH-induced I^- uptake in MCF-7 cells (data not shown). Hence, the stimulatory effect of IBMX on I^- transport may be related to the interaction of IBMX with xanthine-sensitive purinergic P2 receptors (31). When we administered ATP along with tRaH, we observed a moderate but statistically significant increase in NIS protein expression (Fig. 4, C and D) and plasma membrane targeting (Fig. 4, E and F), consistent with the increase in I^- uptake (Fig. 4, A and B). Maximal effect was achieved by 500 μM ATP administered for more than 18 h (Fig. 4, A–F). ATP (500 μM) administered alone, without tRa or hydrocortisone, did not induce functional NIS expression in MCF-7 cells (data not shown). We measured initial rates of I^- uptake in MCF-7 cells treated with tRaH and ATP and found a similar increase in V_{max} to the one observed in cells treated with tRaH and IBMX (Fig. 4G).

To identify the purinergic receptor(s) involved in mediating ATP stimulation of I^- transport, we administered nonhydrolyzable ATP analogs that exhibit different affinities for various P2 receptors (32) (Fig. 5). All experiments were carried out in tRaH-treated MFC-7 cells. The effect of administering IBMX and ATP together was indistinguishable from the effects of administering IBMX or ATP alone (Fig. 5, A–C). Two ATP analogs were tested, namely ATP-γ-S, which interacts with the P2Y1, P2Y2, P2Y11, and P2Y12 receptors, and ADP-β-S, which interacts with the P2Y1, P2Y11, and P2Y12 receptors. Whereas treatment with 100 μM ATP-γ-S had a stimulatory effect similar to that of 500 μM ATP, 100 μM ADP-β-S had no effect (Fig. 5, A–C). Because ATP-γ-S binds with equally high affinity with both P2Y1 and P2Y2, to determine which of these two receptors was involved, we tested UTP, which interacts with P2Y2 but not with P2Y1. We found that UTP (100 or 500 μM) modestly increased I^- uptake and NIS protein expression (Fig. 5, D–F). This suggests that the receptor involved is P2Y2.

To rule out the possibility that the ATP stimulation of I^- transport was mediated by the ATP metabolite adenosine rather than ATP itself, we tested the effect of adenosine on I^- transport, by using stable adenosine analogs exhibiting different affinities for the various adenosine receptor subtypes. Neither N^6-cyclopentyladenosine, *N*-ethylcarboxamidoadenosine, nor N^6-(3-iodobenzyl)-9[5-(methylcarbamoyl-β-D-ribofuranosyl]-adenine had any effect on tRa- or tRaH-induced functional NIS expression in MCF-7 cells (data not shown). In conclusion, given that a nonhydrolyzable ATP analog mimicked the effect of ATP and adenosine analogs had no effect, these data suggest that the stimulatory effect of ATP on iodide transport is mediated by the interaction of ATP with the purinergic receptor P2Y2, not by adenosine interacting with adenosine receptors.

NIS Regulation Differs Markedly in Thyroid *vs.* Breast Cancer Cells

Functional NIS expression in FRTL-5 cells requires TSH (10, 27), whereas in MCF-7 cells it requires tRa (10). Interestingly, Schmutzler *et al.* (33) have reported that 1 μM tRa actually down-regulated NIS mRNA levels and decreased I^- uptake in FRTL-5 cells*, i.e.* tRa had the opposite effect on NIS in thyroid (FRTL-5) cells compared with its effect in breast (MCF-7) cells. Here we have shown, for the first time, that beyond its effect on NIS mRNA and I^- uptake, tRa also decreased TSH-induced NIS protein expression and plasma membrane targeting in FRTL-5 cells (Fig. 6, A–C). Hydrocortisone, for its part, has been reported to lower TSH-induced functional NIS expression in thyroid cells (34), an observation we have confirmed by measuring decreased TSH-induced steady-state I^- uptake in FRTL-5 cells in response to hydrocortisone treatment (data not shown). In contrast, we showed that hydrocortisone markedly increased tRa-induced I^- uptake in MCF-7 cells (Fig. 1). NIS expression in thyroid and breast cancer cells is regulated by different purinergic signals. The presence of multiple P2Y receptor subtypes has been proven in FRTL-5 cells, and these receptors have been suggested to participate in regulation of DNA synthesis (35, 36).

ATP increased NIS expression in MCF-7 cells (Figs. 4 and 5) probably via P2Y2 receptors. Surprisingly, when we tested the effect of ATP on NIS expression in FRTL-5 cells, we found that, in contrast to MCF-7 cells, ATP significantly reduced TSH-induced NIS protein expression, plasma membrane targeting, and steady-state I^- uptake (Fig. 6, A–C). IBMX increased I^- uptake both in FRTL-5 (30) and MCF-7 cells (Fig. 4), probably by different mechanisms.

Other than TSH, I^- is the main regulator of NIS expression and thus of its own transport in the thyroid.

protein (20 μg) was loaded onto each lane. *Middle panels*, Equal loading was assessed by reprobing the same blot with an Ab against the α-subunit of the Na^+/K^+ ATPase. *Bottom panel*, NIS protein expression was quantitated using ImageQuant software and standardized for the loading control. E and F, Plasma membrane targeting of NIS in MCF-7 cells treated with tRaH and with the indicated concentrations of ATP for 48 h (panel E), or with 5×10^{-4} M ATP for the indicated times (panel F). *Upper panel*, Immunoblot analysis of biotinylated cell surface polypeptides using 2 nM anti-hNIS Ab, carried out as described in *Materials and Methods. Middle panel*, Immunoblot analysis of biotinylated cell surface polypeptides using an Ab against the α-subunit of the Na^+/K^+ ATPase. *Bottom panel*, NIS plasma membrane localization was quantified by densitometry using ImageQuant software and standardized for plasma membrane-localized α-subunit of the Na^+/K^+ ATPase. G, IBMX and ATP increase to a similar extent the V_{max} of NIS-mediated I^- transport in tRaH-treated MCF-7 cells, without changing the K_m of the transporter for I^-. Initial rates (2-min time points) of I^- uptake were determined at the indicated concentrations of I^- as described in *Materials and Methods*. Calculated curves (*smooth lines*) were generated using the equation $v = V_{max}\cdot[I]/(K_m+[I])$ with Gnuplot software.

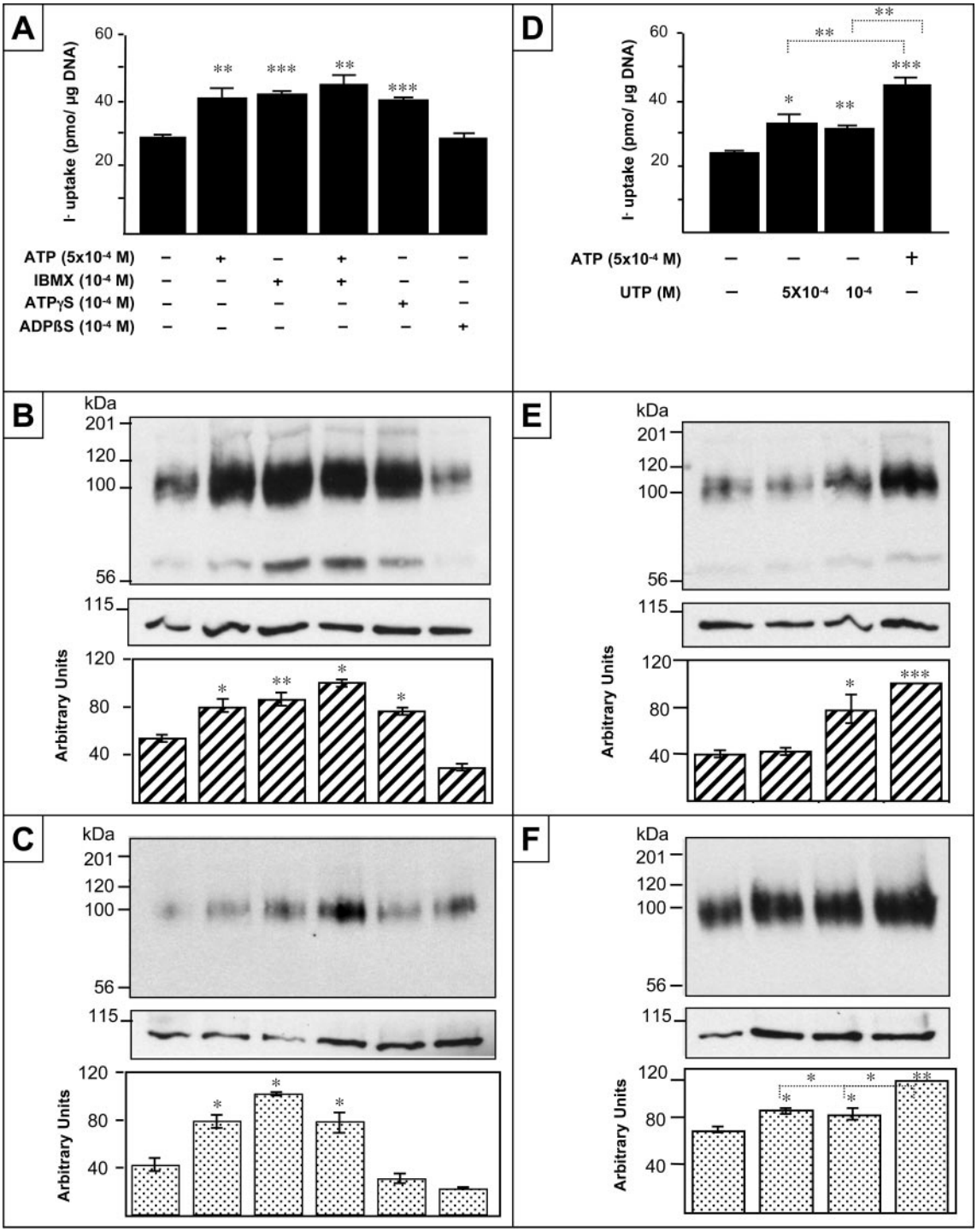

Fig. 5. Effect of Various P2 Receptor-Specific Ligands on tRaH-Induced I^- Uptake in MCF-7 Cells

A and D, Steady-state I^- uptake of MCF-7 cells treated 48 h with 100 μM ATP-γ-S (a P2Y1, P2Y2, P2Y11, and P2Y12 agonist) increased tRaH-induced steady-state I^- uptake of MCF-7 cells to an extent similar to that of ATP (500 μM) or IBMX (100 μM); in contrast, ADP-β-S (a P2Y1, P2Y11, and P2Y12 agonist) exhibited no effect (panel A). UTP (a P2Y2 agonist) only moderately increased tRaH-induced steady-state I^- uptake in MCF-7 cells. All cells were treated with tRaH; only ATP, IBMX, ATP-γ-S, ADP-β-S (panel A), and UTP (panel D) treatments are indicated. Cells were incubated for 30 min with 20 μM $Na^{125}I$ and assayed as described in *Materials and Methods.* B and E, Total NIS expression in tRaH-treated MCF-7 cells after administration of various P2 receptor ligands. *Upper panels*, MCF-7 cells were treated for 48 h with tRaH and either ATP (500 μM), IBMX (100 μM), ATP-γ-S (100 μM), ADP-β-S (100 μM), or UTP (100 and 500 μM) for 48 h, as indicated. Cells were lysed and subjected to immunoblot analysis with 4 nM anti-hNIS Ab. Total protein (20 μg) was loaded onto each lane. *Middle panels*, Equal loading was assessed by reprobing the same blot with an Ab against the α-subunit of the Na^+/K^+ ATPase. *Bottom panels*, NIS protein expression was

The Wolff-Chaikoff effect, first described in 1948, is the blocking of thyroid I^- organification (covalent incorporation of I^- into thyroglobulin) by high concentrations of I^- itself (37). Shortly after this condition is established, the thyroid gland protects itself against I^- overload by down-regulating the transport of the anion, leading to restoration of I^- organification. This latter physiological phenomenon is called the "escape" from the acute Wolff-Chaikoff effect (38, 39). With the availability of the NIS cDNA and NIS Abs, it was shown that high I^- doses down-regulate NIS protein expression, and consequently I^- transport, mostly by a posttranslational mechanism that remains to be fully characterized (39–42). To examine whether I^- modulates NIS activity in breast epithelial cells, FRTL-5 and MCF-7 cells were incubated with 100 μM $Na^{125}I$ overnight, and then assayed for I^- transport and NIS protein expression. Surprisingly, I^- preincubation had no effect either on I^- transport or NIS protein expression in MCF-7 cells (Fig. 6, D–F, *right panels*). This contrasted both with the expected and previously reported (39–42) inhibition of I^- uptake by I^- preincubation in thyroid cells (Fig. 6D, *left panel*), and with the presently observed decrease in expression at the plasma membrane by I^- preincubation (Fig. 6F, *left panel*), an effect that had not been shown before.

DISCUSSION

NIS-mediated radioiodide treatment of metastatic thyroid cancer after thyroidectomy is the most effective anticancer targeted radiotherapy available today, and it causes only minimal side effects (2). Breast cancer is the only malignancy other than thyroid cancer to have been shown thus far to exhibit endogenous functional NIS expression, not only in primary tumors but also in metastases (4–6). Given the enormous health impact of breast cancer (~200,000 newly diagnosed cases per year in the United States), endogenous NIS expression is a distinct advantage of this disease over other malignancies for the purpose of treating it with radioiodide therapy, because it is a cancer that only requires optimization of its existing intrinsic NIS activity without the need to introduce NIS into tumor cells by means of gene transfer techniques (4–6).

An understanding of NIS regulation is a key requirement for optimizing radioiodide therapy in breast cancer, as has been done in thyroid cancer. Therefore, we have investigated the regulation of NIS activity by a variety of factors in MCF-7 cells, a frequently used *in vitro* model system to study regulatory effects in human breast adenocarcinoma, and observed that NIS regulation in these cells is markedly different from that in thyroid FRTL-5 cells. Kogai *et al.* (10, 43) have demonstrated that tRa (or some tRA analogs, like 9-*cis*-retinoic acid and AGN190168) is an absolute requirement to induce NIS expression in MCF-7 cells, an observation that we have confirmed in this study. In contrast, Arturi *et al.* (44) reported that iodide uptake in MCF-7 cells could be induced by insulin, IGF-I, IGF-II, and prolactin in the absence of tRa, a finding that we could not reproduce either under serum-starved or nonstarved conditions. Moreover, when we added these growth factors simultaneously with tRa or tRaH, insulin or IGF-I actually had a slight inhibitory effect (data not shown).

Being convinced that tRa treatment is an absolute requirement to elicit NIS expression in MCF-7 cells, we sought to test modulators that might increase the tRa effect, such as hydrocortisone, a hormone that induces milk protein synthesis in cell and organ cultures when given in combination with insulin and prolactin (23–25). Indeed, we found that hydrocortisone significantly enhanced tRa-induced I^- transport in MCF-7 cells (Fig. 1A). In a time- and dose-dependent fashion, hydrocortisone increased the V_{max} (Fig. 1, C and D) of tRa-induced I^- transport in MCF-7cells by increasing total (Fig. 1E) and cell surface NIS protein expression (Fig. 1F), without affecting I^- efflux (Fig. 1B). Hydrocortisone alone (*i.e*. without tRa) did not have a significant effect (Fig. 1A). Our observations confirm and extend those from a recent report by Kogai *et al.* (43) showing that dexamethasone increased tRa-induced I^- uptake in MCF-7 cells. These authors suggested that hydrocortisone stabilizes tRa-induced NIS mRNA (43). Future studies are necessary to elucidate the mechanism of the tRa-hydrocortisone effect.

MCF-7 cells are known to be heterogenous (26). When treated with tRa, only 10% of cells exhibited NIS expression (Fig. 1K). In contrast, when cells were treated with the tRaH combination, as many as 30% of the cells expressed NIS protein (Fig. 1L). This clearly indicates that hydrocortisone significantly enhances the turn-on effect of tRa on NIS expression. Not much is known about the mechanism by which tRa upregulates NIS expression in MCF-7 cells. Recently, Dentice *et al.* (45) observed that, in MCF-7 cells, tRa treatment induces the expression of Nkx-2.5, a cardiac homeobox transcription factor that, in turn, is a potent inducer of the NIS promoter.

quantitated using ImageQuant software and standardized for the loading control. C and F, Plasma membrane targeting of NIS in tRaH- and P2 receptor agonist-treated MCF-7 cells. *Upper panels*, Immunoblot analysis of biotinylated cell surface polypeptides using 4 nM anti-hNIS Ab, carried out as described in *Materials and Methods. Middle panels*, Immunoblot analysis of biotinylated cell surface polypeptides using an Ab against the α-subunit of the Na^+/K^+ ATPase. *Bottom panels*, NIS plasma membrane localization was quantified by densitometry using ImageQuant software and standardized for plasma membrane-localized α-subunit of the Na^+/K^+ ATPase.

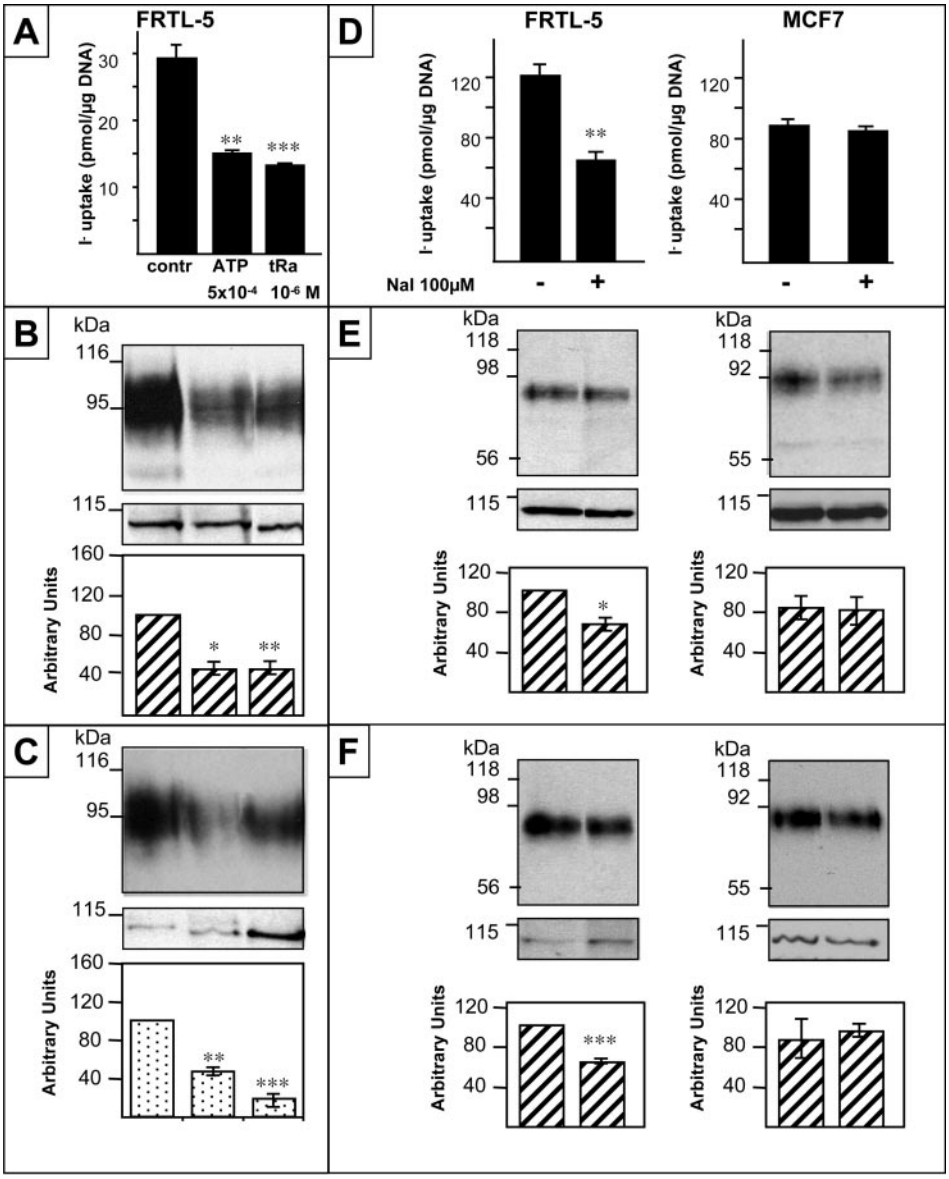

Fig. 6. NIS Regulation Differs Markedly in MCF-7 and FRTL-5 Cells

A, Steady-state I^- uptake is reduced in FRTL-5 cells upon addition of TSH combined with either 500 μM ATP or 1 μM tRa. FRTL-5 cells were kept for 6 d without TSH; TSH was then added either with ATP or tRa for 48 h. B, Both ATP and tRa decrease TSH-induced NIS protein expression in FRTL-5 cells. *Upper panel*, Immunoblot analysis of rNIS expression (20 μg total protein/lane) in FRTL-5 cells kept in the absence of TSH for 6 d; TSH was added in combination with either ATP or tRa for 48 h. *Middle panel*, Loading control (tubulin). *Bottom panel*, NIS protein expression was quantitated using ImageQuant software and standardized for the loading control. C, Plasma membrane targeting of NIS in FRTL-5 cells after TSH induction and treatment with ATP or tRa using anti-rNIS polyclonal Ab. *Upper panels*, Immunoblot analysis of biotinylated cell surface polypeptides using 4 nM anti-rNIS Ab, carried out as described in *Materials and Methods. Middle panel*, Immunoblot analysis of biotinylated cell surface polypeptides using an Ab against the α-subunit of the Na^+/K^+ ATPase. *Bottom panel*, NIS plasma membrane localization was quantified by densitometry using ImageQuant software and standardized for plasma membrane-localized α-subunit of the Na^+/K^+ ATPase. D, Steady-state I^- uptake in FRTL-5 and MCF-7 cells after preincubation with 100 μM $Na^{125}I$. FRTL-5 cells were incubated for 6 h and MCF-7 cells were incubated for 12 h in media containing 100 μM $Na^{125}I$ overnight or for 30 min; accumulated I^- was determined as described in *Materials and Methods.* E, Total NIS protein expression in FRTL-5 and MCF-7 cells after 100 μM NaI treatment. *Upper panel*, Immunoblot analysis of NIS expression (20 μg total protein/lane) in FRTL-5 and MCF-7 cells treated with 100 μM NaI for 6 or 12 h, respectively. *Middle panel*, Loading control (FRTL-5 cells, tubulin; MCF-7 cells, α-subunit of the Na^+/K^+ ATPase). *Bottom panel*, NIS protein expression was quantitated using ImageQuant software and standardized for the loading control. F, Plasma membrane targeting of NIS in FRTL-5- and tRaH-treated MCF-7 cells after administration of 100 μM NaI. *Upper panel*, Immunoblot analysis of biotinylated cell surface polypeptides using 2 nM anti-hNIS Ab or anti-rNIS Ab, carried out as described in *Materials and Methods. Middle panel*, Immunoblot analysis of biotinylated cell surface polypeptides using an Ab against the α-subunit of the Na^+/K^+ ATPase. *Bottom panel*, NIS plasma membrane localization was quantitated by densitometry using ImageQuant software and standardized for plasma membrane localized α-subunit of the Na^+/K^+ ATPase. Contr, Control.

In the thyroid, a major modulator that markedly up-regulates NIS expression is cAMP (27–29). Hence, we tested 8-Br cAMP, a membrane-permeable analog of cAMP; forskolin, an adenyl cyclase activator; and IBMX, a phosphodiesterase inhibitor in MCF-7 cells. All three lead to increased intracellular cAMP levels. Interestingly, far from stimulating it, 8-Br-cAMP caused a very slight decrease in both tRa- and tRaH-induced I^- uptake. This finding alone indicates that cAMP does not play the same up-regulating role in NIS expression in breast cancer cells as it does in thyroid cells (15, 27). Kogai *et al.* (10) reported no effect of forskolin alone (*i.e.* without tRa) on NIS expression in MCF-7 cells, an observation we have confirmed (data not shown), demonstrating that, in the absence of tRa, cAMP alone does not up-regulate NIS in these cells. Like 8-Br-cAMP, forskolin also caused a decrease in both tRa- and tRaH-induced I^- uptake in MCF-7 cells (Fig. 3D), although the decrease was much more pronounced than that with 8-Br-cAMP, and most likely was not due to higher intracellular cAMP levels. In stark contrast, Arturi *et al.* (44) reported that forskolin and dibutyryl-cAMP treatment produced a minimal increase of I^- uptake in MCF-7 cells.

Given that both 8-Br-cAMP and forskolin caused a decrease in both tRa- and tRaH-induced NIS activity, it was most surprising to find that IBMX significantly increased, rather than decreased, I^- uptake (both initial rates and steady state) and NIS protein expression in these cells (Fig. 3), an effect that was clearly independent of phosphodiesterase inhibition and of cAMP levels.

Although the above observations appear to be in conflict with a report by Knostman *et al.* (46) stating that cAMP induces NIS expression in breast cancer, there is no real discrepancy with our findings: these authors observed that 8-Br-cAMP treatment stimulated NIS mRNA expression in MCF-7 cells, but there was no concomitant increase in I^- uptake. Like Kogai *et al.* (10) and our group, Knostman *et al.* (46) also found that forskolin alone did not increase I^- uptake in MCF-7 cells. Thus, in light of our current findings, we conclude that cAMP does not induce NIS protein expression and function in MCF-7 cells. In contrast, IBMX up-regulates both I^- uptake and NIS protein expression in these cells, albeit by a mechanism that does not involve either phosphodiesterase inhibition or an increase in intracellular cAMP levels. Therefore, we suggest that the up-regulating effect of IBMX on NIS expression in MCF-7 cells, also reported by Knostman *et al.,* is unrelated to cAMP.

Having ruled out the possibility that the surprising non-cAMP-dependent stimulatory effect of IBMX on NIS expression was mediated by an increase in cGMP (data not shown), and considering that the effect was clearly not mediated by phosphodiesterase inhibition, we analyzed the potential involvement of purinergic signaling. Methylxanthines are known antagonists of adenosine receptors, and the possible existence of methylxanthine-sensitive purinergic receptors has also been described (31). We found that ATP, like IBMX, significantly increased tRaH-induced I^- uptake in MCF-7 cells. A given epithelial cell type commonly expresses a mixture of various purinergic receptors, and the combination of the different receptors that are present determines how the signal is transduced from the extracellularly released ATP and/or its metabolites. Purinergic receptors are divided into two classes: G protein-coupled P1 adenosine receptors and nucleotide P2 receptors, which bind ATP, ADP, UTP, and UDP. Yoshioka *et al.* (47) have recently reported that the A1 and P2Y1 receptors can oligomerize, thus resulting in A1 receptor ligand-induced P2Y1 receptor signaling. In addition to the versatility of receptors capable of transmitting purinergic signals, other factors influencing their signaling are the metastable nature of ATP and the role of its metabolites. Extracellularly, ATP is degraded rapidly by different ectoenzymes, yielding ADP, 5′-AMP, and adenosine. We observed no effect of stable adenosine analogs on tRaH-induced I^- uptake (data not shown), ruling out the possibility that IBMX acts through adenosine receptors or that the effect of ATP is mediated by its metabolite adenosine.

The complex interactions described above make it difficult to identify with certainty the purinergic receptor that mediates the stimulation of NIS expression by ATP. Still, we addressed this point by administering various ATP analogs and other nucleotides with different receptor specificities and determining their effectiveness in stimulating I^- transport in MCF-7 cells (Fig. 5). ATP and UTP are known to elevate intracellular calcium and stimulate proliferation via activation of the P2Y2 receptor in MCF-7 cells. These cells express P2Y2 receptors and proliferate in response to both ATP and UTP (48). We found that the nonhydrolyzable ATP analog ATPγS was as effective as ATP itself in stimulating I^- transport, whereas UTP was noticeably less so and ADPβS had no effect (Fig. 5). These findings suggest that the receptor involved is probably P2Y2 (32).

We have previously reported that functional NIS expression in the mammary gland appears during the second half of gestation and is maintained thereafter by suckling during lactation (4). We have also shown that, whereas oxytocin alone up-regulates NIS expression in the mammary glands of nubile mice, the combination of estrogen, oxytocin, and prolactin induces the highest NIS protein expression (4). The lack of any effect of prolactin and oxytocin on NIS expression in MCF-7 cells (data not shown) could be explained either by the malignant status of these cells or by the absence of the required microenvironment, particularly myoepithelial cells. Furthermore, it has been observed that tRa down-regulates prolactin receptor expression in MCF-7 cells (49). In these cells, ATP and UTP promote cell proliferation via stimulation of the P2Y2 receptors (48, 50). In the lactating mammary gland, P2Y2-expressing secretory epithelial and P2Y1-expressing myoepithelial cells are believed to

interact via released ATP to enhance milk ejection (51–53). Mechanical stretch (*e.g*. alveoli filling with milk) induces ATP release from epithelial cells (51–53). Oxytocin, which by itself is able to up-regulate NIS expression in nubile mice, most likely exerts its effect through the myoepithelial cells. Myoepithelial cell contraction in response to oxytocin leads to ATP release, which probably increases NIS expression and I^- transport into the epithelial cells. Our study of the purinergic regulation of NIS expression, reported here for the first time, shows that ATP up-regulates NIS expression in MCF-7 cells (Fig. 4) but decreases it in FRTL-5 cells (Fig. 6, A–C). The main requirement for NIS expression in FRTL-5 cells is TSH, whereas in MCF-7 cells it is tRa. TSH has no effect in MCF-7 cells. In FRTL-5 cells, cAMP is the main positive regulator of NIS expression, but in MCF-7 cells, cAMP had no effect on NIS expression (Fig. 3, A–C). Clearly, the regulation of NIS expression is tissue specific, and some regulatory factors have opposite effects on NIS expression in different tissues. tRa significantly decreased the amount of total and plasma membrane-localized NIS protein in FRTL-5 cells (Fig. 6, A–C); in contrast, tRa had the opposite effect in MCF-7 cells (Fig. 1). Hydrocortisone, which is added to the FRTL-5 media to improve surface attachment (34), decreases TSH-induced I^- uptake in FRTL-5 cells, whereas it significantly enhanced tRa-induced NIS expression in MCF-7 cells (Fig. 1). It has long been known that I^- at high concentrations down-regulates its own transport in thyroid cells. Here we have shown, for the first time, that I^-, even at high concentrations, had no effect on its own transport in MCF-7 cells (Fig. 6).

In conclusion, having previously reported NIS protein expression in more than 80% of human breast cancers (4) and functional NIS expression in human breast cancer metastases *in vivo* (6) without expression in healthy nonlactating mammary tissue (4), we have now demonstrated that: 1) hydrocortisone and ATP stimulate tRa-induced functional NIS expression in human breast carcinoma MCF-7 cells; 2) IBMX increases tRa-induced NIS expression in these cells by a purinergic signaling pathway; and 3) regulatory factors of NIS expression exert different and sometimes even opposite effects on breast cancer as compared with thyroid cells. The differences in regulatory mechanisms of NIS expression between these tissues provide a key advantage for the development of selective treatment strategies that would destroy breast cancer cells without harming the thyroid. As MCF-7 and FRTL-5 cells have been extensively used for *in vitro* investigations of *in vivo* regulatory processes of breast cancer and healthy thyroid, respectively, data obtained in these cell lines are widely regarded as being potentially physiologically relevant. Thus, our results may be a significant step toward the goal of effectively applying radioiodide in the diagnosis and therapy of breast cancer. Nevertheless, these findings on selective up-regulation of NIS expression in breast cancer cells by tRa, hydrocortisone, and IBMX will require subsequent *in vivo* validation in future animal and, eventually, human studies.

MATERIALS AND METHODS

Materials

All-trans-retinoic acid, hydrocortisone, 8-Br-cAMP, 8-bromoguanosine-3′,5′-cyclomonophosphate sodium salt (8-bromo-cGMP), IBMX, ATP, ATP-γ-S, ADP-β-S, UTP, adenosine, N^6-cyclopentyladenosine, N^6-(3-iodobenzyl)-9[5-(methylcarbamoyl-β-D-ribofuranosyl]adenine, *N*-ethylcarboxamidoadenosine, estradiol, human recombinant prolactin, and oxytocin were from Sigma-Aldrich (St. Louis, MO). Forskolin was from Calbiochem (San Diego, CA).

Cell Culture

MCF-7 cells (lot 2188915) were purchased from American Type Culture Collection (Manassas, VA), and they were grown in Eagle's MEM with Earle's balanced salt solution and 2 mM L-glutamine, containing 1 mM sodium pyruvate, 0.1 mM nonessential amino acids, 1.5 g/liter sodium bicarbonate, and supplemented with 0.01 mg/ml bovine insulin and 10% fetal bovine serum. Before (48 h) and during the hormonal treatments, the medium was switched to medium containing only 2.5% charcoal dextran-stripped serum (Gemini Bio-Products, Woodland, CA). FRTL-5 cells were maintained as described previously (15).

Iodide Uptake

After the culture medium was aspirated, cells were washed twice with 1 ml of a modified Hanks' balanced salt solution (buffered HBSS) with the following composition: 137 mM NaCl, 5.4 mM KCl, 1.3 mM $CaCl_2$, 0.4 mM $MgSO_4 \cdot 7\ H_2O$, 0.5 mM $MgCl_2$, 0.4 mM $Na_2HPO_4 \cdot 7\ H_2O$, 0.44 mM KH_2PO_4, and 5.55 mM glucose with 10 mM HEPES buffer (pH 7.3). Cells grown in 24-well plates were incubated with buffered HBSS containing 20 μM NaI supplemented with 10 μCi/μl carrier-free $Na^{125}I$ to give a specific activity of 100 mCi/mmol. For steady-state experiments, incubations proceeded at 37 C for 45 min in a humidified atmosphere and were terminated by aspirating the radioactive medium and washing twice with 1 ml ice-cold HBSS. For kinetic analysis, cells were incubated for 2 min with 0.625, 1.25, 2.5, 5, 10, 20, 40, or 80 μM NaI, and uptake reactions were terminated as indicated above. Data were processed using the equation: $v = V_{max} \cdot [I]/(K_m + [I])$. To assess Na^+ dependence of I^- uptake, cells were incubated for 2 min with 0, 5, 10, 20, 30, 40, 80, or 140 mM NaCl; isotonicity was maintained constant with choline Cl. Na^+ dependence data were analyzed using the equation: $v = V_{max} \cdot [Na^+]^2/K_m + [Na^+]^2$. Data were fitted by nonlinear least squares using Gnuplot software (www.gnuplot.info). Nonspecific background, as measured in nontreated cells, was subtracted.

To determine the amount of ^{125}I accumulated in the cells, 500 μl 95% ethanol was added to each well for 20 min at 4 C and then quantitated in a γ-counter. The DNA content of each well was determined on the material not extracted by ethanol after trichloroacetic acid precipitation, by the diphenylamine method, as previously described (54). I^- uptake was expressed as picomoles per μg DNA. All parameters were determined at least in triplicate.

Immunoblot Analysis of Total and Biotinylated Plasma Membrane Proteins

Cells were grown in six-well plates to 80% confluence. Cells were rinsed at 4 C twice with PBS/Ca^{2+}/Mg^{2+} (138 mM NaCl;

2.7 mM KCl; 1.5 mM KH_2PO_4; 9.6 mM Na_2HPO_4; 1 mM $MgCl_2$; 0.1 mM $CaCl_2$, pH 7.4). Cells were next incubated with 500 μl/well of a solution containing 1.5 mg/ml sulfo-NH-SS-biotin (Pierce Chemical Co., Rockford, IL) in biotinylation buffer [HEPES 20 mM (pH 8.5), $CaCl_2$ 2 mM, NaCl 150 mM] for 20 min at 4 C with gentle shaking. The biotinylation solution was removed by two washes in PBS Ca^{2+}/Mg^{2+} containing 100 mM glycine. Cells were lysed with 1 ml of lysis buffer (50 mM Tris-HCl, pH 7.5; 150 mM NaCl; 5 mM EDTA; 1% Triton X-100; 1% sodium dodecyl sulfate; protease inhibitors) at 4 C for 15 min. A 200-μl aliquot was taken for assessing total NIS expression by immunoblot. The remaining cell lysate (800 μl) was incubated overnight at 4 C with 50 μl of streptoavidin agarose beads (Pierce). Beads were centrifuged at 5000 $\times$ *g* for 2 min and rinsed three times with lysis buffer, twice with high-salt, and once with low-salt solution. Adsorbed proteins were eluted from the beads with sample buffer containing 10 mM dithiothreitol, at 75 C for 5 min, and analyzed by immunoblot. Ab purification was performed as described previously (17).

PAGE and electroblotting to nitrocellulose were performed as previously described (17). Immunoblot analysis was also carried out as described (17), with affinity-purified 4 nM anti-human NIS or 4 nM antirat NIS Ab, and a 1:2000 dilution of a horseradish peroxidase-linked donkey antirabbit IgG (Chemicon, Temecula, CA). Both incubations were performed for 1 h. Proteins were visualized by the enhanced chemiluminescence Western blot detection system (Amersham Pharmacia Biotech, Arlington Heights, IL). Equal loading was assessed by reprobing the same blot with a mAb against the α-subunit of the Na^+/K^+ ATPase (Affinity BioReagents, Inc., Golden, CO). Protein expression was quantitated using ImageQuant software (Molecular Dynamics, Inc., Sunnyvale, CA) and standardized for the loading control.

Immunofluorescence Analysis

MCF-7 cells were seeded onto polylysine-coated cover slips. They were fixed with 2% paraformaldehyde for 30 min at room temperature and then rinsed with PBS containing 0.1 mM $CaCl_2$ and 1 mM $MgCl_2$, subsequently referred to as PBS-C-M. Cells were permeabilized with PBS-C-M-0.2% BSA-0.1% Triton for 10 min and then quenched with 50 mM NH_4Cl in PBS-C-M for 10 min. Cells were rinsed with PBS-C-M-BSA-Triton and incubated for 1 h at room temperature with 4 nM affinity-purified anti-hNIS Ab in PBS-C-M-BSA-Triton. Subsequently, cells were washed three times for 10 min with PBS-C-M-BSA-Triton, incubated for 1 h in the dark with antirabbit fluorescein-conjugated secondary Ab (Vector Laboratories, Inc., Burlingame, CA) (1:1000 dilution), and washed as above. Cover slips were mounted onto slides with Slow Fade antifade reagent (Molecular Probes, Inc., Eugene, OR), sealed with quick-dry nail polish, and allowed to dry in the dark for 2 h at room temperature and then stored at 4 C in the dark. Cells were visualized in a Bio-Rad Radiance 2000 Laser Scanning Confocal Microscope (Bio-Rad Laboratories, Inc., Hercules, CA).

Flow Cytometry

MCF-7 cells were detached with trypsin, counted, fixed in PBS containing 2% paraformaldehyde, and then permeabilized with 0.2% saponin in PBS supplemented with 0.1% BSA and transferred into 5-ml polystyrene tubes (200,000 cells per tube). Cells were incubated for 1 h at room temperature with 100 μl PBS-0.1% BSA-0.2% Sap containing 4 nM anti-hNIS Ab. Cells were washed with 1 ml PBS-BSA-saponin and centrifuged as above. Next, they were incubated for 30 min at room temperature in the dark with fluorescein-conjugated antirabbit IgG (Vector Laboratories) at a 1:1000 dilution in the same buffer. Cells were washed once again, centrifuged, and resuspended in 300 μl PBS. The fluorescence of 10,000 cells per tube was assayed by a FACScan flow cytometer (Becton Dickinson and Co., Franklin Lakes, NJ).

Statistical Analysis

Statistical analyses were performed using Student's *t* test. Each experimental condition was compared with its respective control group; *P* values below 0.05, below 0.01, and below 0.001 are represented as *, **, and ***, respectively, in all figures.

Acknowledgments

We thank the members of the Carrasco laboratory for critical reading of the manuscript.

Received September 13, 2005. Accepted January 17, 2006.

Address all correspondence and requests for reprints to: Nancy Carrasco, Department of Molecular Pharmacology, Albert Einstein College of Medicine, 1300 Morris Park Avenue, Bronx, New York 10461. E-mail: carrasco@aecom.yu.edu.

This work was supported by National Institutes of Health Grant CA098390 (to N.C.). O.D. was supported, in part, by a postdoctoral award from the Department of Defense (DAMD17-0010127).

Disclosure summary: all authors have nothing to declare.

REFERENCES

1. Milenic DE, Brady ED, Brechbiel MW 2004 Antibody-targeted radiation cancer therapy. Nat Rev Drug Discov 3:488–499
2. Mazzaferri EL 2000 Thyroid diseases: tumors. Radioiodine and other treatment and outcomes. In: Braverman LE, Utiger RD, eds. Werner, Ingbar's the thyroid. 8th ed. Baltimore: Lippincott Williams & Wilkins; 904–930
3. Seidlin SM, Marinelli LD, Oshry E 1946 Radioactive iodine therapy. JAMA 132:838–847
4. Tazebay UH, Wapnir IL, Levy O, Dohan O, Zuckier LS, Zhao QH, Deng HF, Amenta PS, Fineberg S, Pestell RG, Carrasco N 2000 The mammary gland iodide transporter is expressed during lactation and in breast cancer. Nat Med 6:871–878
5. Moon DH, Lee SJ, Park KY, Park KK, Ahn SH, Pai MS, Chang H, Lee HK, Ahn IM 2001 Correlation between 99mTc-pertechnetate uptakes and expressions of human sodium iodide symporter gene in breast tumor tissues. Nucl Med Biol 28:829–834
6. Wapnir IL, Goris M, Yudd A, Dohan O, Adelman D, Nowels K, Carrasco N 2004 The Na^+/I^- symporter mediates iodide uptake in breast cancer metastases and can be selectively down-regulated in the thyroid. Clin Cancer Res 10:4294–4302
7. Spitzweg C, Dietz AB, O'Connor MK, Bergert ER, Tindall DJ, Young CY, Morris JC 2001 In vivo sodium iodide symporter gene therapy of prostate cancer. Gene Ther 8:1524–1531
8. Dingli D, Diaz RM, Bergert ER, O'Connor MK, Morris JC, Russell SJ 2003 Genetically targeted radiotherapy for multiple myeloma. Blood 102:489–496
9. Faivre J, Clerc J, Gerolami R, Herve J, Longuet M, Liu B, Roux J, Moal F, Perricaudet M, Brechot C 2004 Long-term radioiodine retention and regression of liver cancer after sodium iodide symporter gene transfer in Wistar rats. Cancer Res 64:8045–8051

10. Kogai T, Schultz JJ, Johnson LS, Huang M, Brent GA 2000 Retinoic acid induces sodium/iodide symporter gene expression and radioiodide uptake in the MCF-7 breast cancer cell line. Proc Natl Acad Sci USA 97: 8519–8524
11. Kogai T, Kanamoto Y, Che LH, Taki K, Moatamed F, Schultz JJ, Brent GA 2004 Systemic retinoic acid treatment induces sodium/iodide symporter expression and radioiodide uptake in mouse breast cancer models. Cancer Res 64:415–422
12. Dai G, Levy O, Carrasco N 1996 Cloning and characterization of the thyroid iodide transporter. Nature 379: 458–460
13. Spitzweg C, Joba W, Eisenmenger W, Heufelder AE 1998 Analysis of human sodium iodide symporter gene expression in extrathyroidal tissues and cloning of its complementary deoxyribonucleic acids from salivary gland, mammary gland, and gastric mucosa. J Clin Endocrinol Metab 83:1746–1751
14. Dohan O, De la Vieja A, Paroder V, Riedel C, Artani M, Reed M, Ginter CS, Carrasco N 2003 The sodium/iodide symporter (NIS): characterization, regulation, and medical significance. Endocr Rev 24:48–77
15. Riedel C, Levy O, Carrasco N 2001 Post-transcriptional regulation of the sodium/iodide symporter by thyrotropin. J Biol Chem 276:21458–21463
16. Dohan O, Carrasco N 2003 Advances in Na(+)/I(−) symporter (NIS) research in the thyroid and beyond. Mol Cell Endocrinol 213:59–70
17. Levy O, Dai G, Riedel C, Ginter CS, Paul EM, Lebowitz AN, Carrasco N 1997 Characterization of the thyroid Na+/I− symporter with an anti-COOH terminus antibody. Proc Natl Acad Sci USA 94:5568–5573
18. Eskandari S, Loo DD, Dai G, Levy O, Wright EM, Carrasco N 1997 Thyroid Na+/I− symporter. Mechanism, stoichiometry, and specificity. J Biol Chem 272: 27230–27238
19. Zuckier LS, Dadachova E, Dohan O, Carrasco N 2001 The endogenous mammary gland Na(+)/I(−) symporter may mediate effective radioiodide therapy in breast cancer. J Nucl Med 42:987–988
20. Carlin S, Mairs RJ, Welsh P, Zalutsky MR 2002 Sodium-iodide symporter (NIS)-mediated accumulation of [(211)At]astatide in NIS-transfected human cancer cells. Nucl Med Biol 29:729–739
21. Wapnir IL, van de Rijn M, Nowels K, Amenta PS, Walton K, Montgomery K, Greco RS, Dohan O, Carrasco N 2003 Immunohistochemical profile of the sodium/iodide symporter in thyroid, breast, and other carcinomas using high density tissue microarrays and conventional sections. J Clin Endocrinol Metab 88:1880–1888
22. Robbins RJ, Tuttle RM, Sonenberg M, Shaha A, Sharaf R, Robbins H, Fleisher M, Larson SM 2001 Radioiodine ablation of thyroid remnants after preparation with recombinant human thyrotropin. Thyroid 11:865–869
23. Rosen JM, Wyszomierski SL, Hadsell D 1999 Regulation of milk protein gene expression. Annu Rev Nutr 19: 407–436
24. Topper RJ, Oka T, Vonderhaar BK 1975 Techniques for studying development of normal mammary epithelial cells in organ culture. Methods Enzymol 39:443–454
25. Danielson KG, Oborn CJ, Durban EM, Butel JS, Medina D 1984 Epithelial mouse mammary cell line exhibiting normal morphogenesis in vivo and functional differentiation in vitro. Proc Natl Acad Sci USA 81:3756–3760
26. Lacroix M, Leclercq G 2004 Relevance of breast cancer cell lines as models for breast tumours: an update. Breast Cancer Res Treat 83:249–289
27. Weiss SJ, Philp NJ, Ambesi-Impiombato FS, Grollman EF 1984 Thyrotropin-stimulated iodide transport mediated by adenosine 3′,5′-monophosphate and dependent on protein synthesis. Endocrinology 114:1099–1107
28. Ohno M, Zannini M, Levy O, Carrasco N, di Lauro R 1999 The paired-domain transcription factor Pax8 binds to the upstream enhancer of the rat sodium/iodide symporter gene and participates in both thyroid-specific and cyclic-AMP-dependent transcription. Mol Cell Biol 19: 2051–2060
29. De La Vieja A, Dohan O, Levy O, Carrasco N 2000 Molecular analysis of the sodium/iodide symporter: impact on thyroid and extrathyroid pathophysiology. Physiol Rev 80:1083–1105
30. Marcocci C, Fenzi GF, Grollman EF 1987 Role of the adenylate cyclase-cAMP system on TSH-stimulated thyroid cell growth. Acta Endocrinol Suppl (Copenh) 281: 246–251
31. Communi D, Janssens R, Suarez-Huerta N, Robaye B, Boeynaems JM 2000 Advances in signalling by extracellular nucleotides. the role and transduction mechanisms of P2Y receptors. Cell Signal 12:351–360
32. Schwiebert EM, Zsembery A 2003 Extracellular ATP as a signaling molecule for epithelial cells. Biochim Biophys Acta 1615:7–32
33. Schmutzler C, Winzer R, Meissner-Weigl J, Kohrle J 1997 Retinoic acid increases sodium/iodide symporter mRNA levels in human thyroid cancer cell lines and suppresses expression of functional symporter in nontransformed FRTL-5 rat thyroid cells. Biochem Biophys Res Commun 240:832–838
34. Saji M, Kohn LD 1990 Effect of hydrocortisone on the ability of thyrotropin to increase deoxyribonucleic acid synthesis and iodide uptake in FRTL-5 rat thyroid cells: opposite regulation of adenosine 3′,5′-monophosphate signal action. Endocrinology 127:1867–1876
35. Tornquist K, Ekokoski E, Dugue B 1996 Purinergic agonist ATP is a comitogen in thyroid FRTL-5 cells. J Cell Physiol 166:241–248
36. Ekokoski E, Webb TE, Simon J, Tornquist K 2001 Mechanisms of P2 receptor-evoked DNA synthesis in thyroid FRTL-5 cells. J Cell Physiol 187:166–175
37. Wolff J, Chaikoff IL 1948 Plasma inorganic iodide as a homeostatic regulator of thyroid function. J Biol Chem 174:555–564
38. Braverman LE, Ingbar SH 1963 Changes in thyroidal function during adaptation to large doses of iodide. J Clin Invest 42:1216–1231
39. Eng PH, Cardona GR, Fang SL, Previti M, Alex S, Carrasco N, Chin WW, Braverman LE 1999 Escape from the acute Wolff-Chaikoff effect is associated with a decrease in thyroid sodium/iodide symporter messenger ribonucleic acid and protein. Endocrinology 140: 3404–3410
40. Eng PH, Cardona GR, Previti MC, Chin WW, Braverman LE 2001 Regulation of the sodium iodide symporter by iodide in FRTL-5 cells. Eur J Endocrinol 144:139–144
41. Grollman EF, Smolar A, Ommaya A, Tombaccini D, Santisteban P 1986 Iodine suppression of iodide uptake in FRTL-5 thyroid cells. Endocrinology 118:2477–2482
42. Dohan O, Osborne J, Carrasco N, Surprising new mechanistic insights into the escape from the Wolff-Chaikoff Effect. Program of the 86th Annual Meeting of The Endocrine Society, New Orleans, LA, 2004, p 102 (Abstract OR 21-5)
43. Kogai T, Kanamoto Y, Li AI, Che LH, Ohashi E, Taki K, Chandraratna RA, Saito T, Brent GA 2005 Differential regulation of sodium/iodide symporter gene expression by nuclear receptor ligands in MCF-7 breast cancer cells. Endocrinology 146:3059–3069
44. Arturi F, Ferretti E, Presta I, Mattei T, Scipioni A, Scarpelli D, Bruno R, Lacroix L, Tosi E, Gulino A, Russo D, Filetti S 2005 Regulation of iodide uptake and sodium/iodide symporter expression in the mcf-7 human breast cancer cell line. J Clin Endocrinol Metab 90:2321–2326
45. Dentice M, Luongo C, Elefante A, Romino R, Ambrosio R, Vitale M, Rossi G, Fenzi G, Salvatore D 2004 Transcrip-

tion factor Nkx-2.5 induces sodium/iodide symporter gene expression and participates in retinoic acid- and lactation-induced transcription in mammary cells. Mol Cell Biol 24:7863–7877
46. Knostman KA, Cho JY, Ryu KY, Lin X, McCubrey JA, Hla T, Liu CH, Di Carlo E, Keri R, Zhang M, Hwang DY, Kisseberth WC, Capen CC, Jhiang SM 2004 Signaling through 3′,5′-cyclic adenosine monophosphate and phosphoinositide-3 kinase induces sodium/iodide symporter expression in breast cancer. J Clin Endocrinol Metab 89:5196–5203
47. Yoshioka K, Saitoh O, Nakata H 2001 Heteromeric association creates a P2Y-like adenosine receptor. Proc Natl Acad Sci USA 98:7617–7622
48. Dixon CJ, Bowler WB, Fleetwood P, Ginty AF, Gallagher JA, Carron JA 1997 Extracellular nucleotides stimulate proliferation in MCF-7 breast cancer cells via P2-purinoceptors. Br J Cancer 75:34–39
49. Widschwendter M, Widschwendter A, Welte T, Daxenbichler G, Zeimet AG, Bergant A, Berger J, Peyrat JP, Michel S, Doppler W, Marth C 1999 Retinoic acid modulates prolactin receptor expression and prolactin-induced STAT-5 activation in breast cancer cells in vitro. Br J Cancer 79:204–210
50. Wagstaff SC, Bowler WB, Gallagher JA, Hipskind RA 2000 Extracellular ATP activates multiple signalling pathways and potentiates growth factor-induced c-fos gene expression in MCF-7 breast cancer cells. Carcinogenesis 21:2175–2181
51. Furuya K, Akita K, Sokabe M 2004 [Extracellular ATP mediated mechano-signaling in mammary glands]. Nippon Yakurigaku Zasshi 123:397–402
52. Nakano H, Furuya K, Yamagishi S 2001 Synergistic effects of ATP on oxytocin-induced intracellular Ca2+ response in mouse mammary myoepithelial cells. Pflugers Arch 442:57–63
53. Nakano H, Furuya K, Furuya S, Yamagishi S 1997 Involvement of P2-purinergic receptors in intracellular Ca^{2+} responses and the contraction of mammary myoepithelial cells. Pflugers Arch 435:1–8
54. Dohan O, Gavrielides MV, Ginter C, Amzel LM, Carrasco N 2002 Na(+)/I(−) symporter activity requires a small and uncharged amino acid residue at position 395. Mol Endocrinol 16:1893–1902

Molecular Endocrinology **is published monthly by The Endocrine Society (http://www.endo-society.org), the foremost professional society serving the endocrine community.**